Influences of Madden–Julian Oscillations on the eastern Indian Ocean and the maritime continent

Article *in* Dynamics of Atmospheres and Oceans · August 2010

DOI: 10.1016/j.dynatmoce.2009.12.003

2 authors:

Lei Zhou
Shanghai Jiao Tong University
48 PUBLICATIONS **692** CITATIONS
SEE PROFILE

Raghu Murtugudde
University of Maryland, College Park
285 PUBLICATIONS **10,267** CITATIONS
SEE PROFILE

Dynamics of Atmospheres and Oceans 50 (2010) 257–274

Contents lists available at ScienceDirect

Dynamics of Atmospheres and Oceans

journal homepage: www.elsevier.com/locate/dynatmoce

Influences of Madden–Julian Oscillations on the eastern Indian Ocean and the maritime continent

Lei Zhou*, Raghu Murtugudde

Earth System Science Interdisciplinary Center, College Park, MD, United States

ARTICLE INFO

Article history:
Available online 28 December 2009

Keywords:
Indonesian Throughflow
Madden–Julian Oscillations
Eastern Indian Ocean
Ocean–atmosphere interaction

ABSTRACT

Oceanic response to Madden–Julian Oscillations (MJOs) is studied with satellite data, mooring observations, and reanalysis products to demonstrate that oceanic intraseasonal variabilities are a direct response to the atmospheric intraseasonal forcing. They propagate eastward to the Sumatran coast and southward along the coast to the southeastern Indian Ocean (SEIO) and the maritime continent, as coastal Kelvin waves. MJOs contribute to about 20% of the intraseasonal variabilities in the SEIO and the maritime continent. In addition, MJOs reduce the annual mean Indonesian Throughflow (ITF) and the associated westward temperature advection. However, MJOs only have slight influences on the peak ITF in boreal summer. The importance of INSTANT data is obvious not only for understanding of ITF but also for improving ocean reanalysis and should eventually lead to improved predictive understanding of phenomena such as MJOs.

1. Introduction

As the major intraseasonal oscillations in the ocean–atmosphere coupled system, Madden–Julian Oscillations (MJOs) have a significant impact on the oceanic variabilities in the tropical Indian Ocean, the maritime continent, and the western Pacific Ocean during their eastward propagation. There have been some previous studies on the MJO influence on the open ocean. For example, in the tropical Pacific Ocean, intraseasonal equatorial Kelvin waves and sea surface temperature (SST) anomalies are attributable to MJO forcing as reported with the TOGA-CORE observations (Kessler et al., 1995;

* Corresponding author at: Univ. of Maryland M-Square Research Park, Rm. 3016, 5825 University Research Ct, Ste 4001, College Park, MD 20740-3823, United States. Tel.: +1 301 405 7093.
E-mail address: lzhou@atmos.umd.edu (L. Zhou).

0377-0265/$ – see front matter © 2009 Elsevier B.V. All rights reserved.
doi:10.1016/j.dynatmoce.2009.12.003

Woolnough et al., 2000). In the tropical Indian Ocean, the oceanic intraseasonal variabilities (ISVs) are enhanced due to internal oceanic instabilities and in response to intraseasonal atmospheric forcing (Waliser et al., 2003; Reppin et al., 1999; Sengupta et al., 2001). Schiller and Godfrey (2003) simulated MJO impacts on the oceanic ISVs with an OGCM to conclude that both air–sea heat flux and horizontal advection are important to the mixed layer heat budget in the tropical Indian Ocean. They also highlighted the formation of the barrier layer in the tropical Indian Ocean, mainly due to the heavy precipitation associated with MJOs. Waliser et al. (2003) studied the oceanic response to carefully constructed composite MJOs in the eastern Indian Ocean and the western Pacific Ocean with a layered OGCM. They also emphasized the important role of local heat flux and horizontal advection, especially the meridional advection, in determining SSTs in the eastern tropical Indian Ocean and the western Pacific Ocean. Moreover, they showed that MJOs can lead to low-frequency variations in the Indo-Pacific SSTs. Recently, the MISMO filed experiments (Yoneyama et al., 2008) were conducted to monitor ocean–atmosphere interactions during MJOs. They reported notable oceanic variations in the central Indian Ocean (80.5°E at the equator) associated with the surface winds and precipitation during the observed MJO events, although the physical mechanism for the relations between the oceanic variations and the MJO forcing are still under exploration.

However, in the eastern Indian Ocean off the Sumatran coast and the maritime continent, there are few studies on the oceanic responses to MJO forcing. Actually, the oceanic ISVs in this region are quite energetic. Feng and Wijffels (2002) analyzed satellite altimeter data and attributed the enhanced oceanic ISVs during the second half of the year (boreal summer) to baroclinic instability, which draws most of its energy from the available potential energy associated with the Indonesian Throughflow (ITF). Yu and Potemra (2006) concluded that barotropic and baroclinic instabilities contribute almost equally to the genesis of the oceanic ISVs in the Indo-Australian basin, by analyzing a numerical ocean model. They found that baroclinic instability was sensitive to the warmer and fresher ITF and barotropic instability was attributable to the strong zonal shear between the Eastern Gyral Current and the South Equatorial Current, which is strengthened by the ITF. In addition to the strong dependence on the ITF (Potemra et al., 2002), the oceanic ISVs in the southeastern Indian Ocean (SEIO) also respond to the intraseasonal atmospheric forcing (Sprintall et al., 2000; Iskandar et al., 2006), which is the focus of this study. With satellite data, mooring observations, and reanalysis products, we intend to quantify the contribution of MJO influence to the oceanic ISVs in the eastern Indian Ocean and the maritime continent.

Since the SEIO is the entrance for the ITF to the Indian Ocean, the variations in the SEIO are likely to influence the strength of ITF. There have been many estimations of the mass and heat fluxes by the ITF, based on various observational projects which were conducted at different times (e.g., Godfrey, 1996; Hautala et al., 2001; Meyers et al., 1995; Susanto and Gordon, 2005; Vranes et al., 2002; Gordon, 2001). The range of the ITF flux is not the focus of this study. But it is evident that the ITF flux varies over a wide range, due to both internal (e.g., tides, internal waves, and the diapycnal mixing; Ffield and Gordon, 1992; Hatayama et al., 1996; Hautala et al., 1996) and external processes (such as surface winds and heat fluxes, ENSO, and Indian Ocean Zonal/Dipole mode; Masumoto, 2002; Meyers, 1996; Murtugudde et al., 1998; Wijffels and Meyers, 2004). If MJOs have detectable influence on the SEIO, it is reasonable to assume that they can also have an influence on the variation of ITF. In fact, Waliser et al. (2003) showed that a large part of the ITF variability was attributable to the constructed composite MJOs in a numerical model.

Therefore, the purpose of this study is to present the MJO influence on the oceanic ISVs in the eastern Indian Ocean, the maritime continent, as well as the relation between MJOs and ITF. In Section 2, data and reanalysis products are introduced. The oceanic response to MJOs is discussed in Section 3 and the MJO influence on the ITF is explored in Section 4. The conclusions and discussion are presented in Section 5.

2. Data

The MJO events are defined with an MJO index, which was created by Wheeler and Hendon (2004) with the daily outgoing longwave radiation (OLR) from NOAA polar-orbiting series of satellites (Liebmann and Smith, 1996) and zonal winds at 850 hPa and 200 hPa from daily NCEP reanalysis

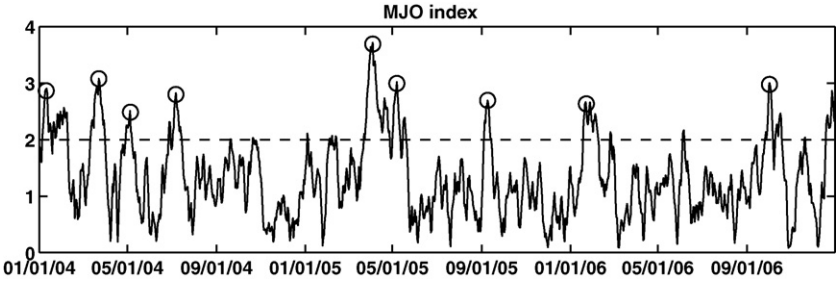

Fig. 1. MJO index calculated following Wheeler and Hendon (2004). The peaks of the significant MJO events with an MJO index larger than 2 are marked with circles.

(Kalnay and Coauthors, 1996). This MJO index has been widely used in the MJO study and has been proven to be capable of capturing the MJO events. Thus, although the quality of NCEP reanalysis is questioned on occasions (e.g., Milliff et al., 2004), especially compared to ERA-40 (Simmons and Gibson, 2000), the MJO index established based on NCEP reanalysis is still used in this study. Note that this MJO index only allows the eastward-propagating events. The independent northward-propagating events (e.g., the event from September 18, 1984 to October 17, 1984) and the westward-propagating events (e.g., the event from August 19, 1982 to September 12, 1982) are excluded (see the categories of the tropical atmospheric ISVs in Wang and Rui, 1990). The amplitude of MJOs is determined with the sum of the squares of the first two leading principal components (PCs) of the combined fields (i.e. MJO index = $PC1^2 + PC2^2$) and a significant MJO event is one with an MJO index larger than 2 (Fig. 1). The phase of MJOs is determined with the angle between PC1 and PC2 (not shown, see Wheeler and Hendon, 2004 for details). In the following calculations, the daily MJO index is used.

Daily AVHRR gridded SSTs from 1985 to 2006 (McClain et al., 1985) are obtained from the Physical Oceanography Distributed Active Archive Center (PO.DAAC). Weekly SSHs from satellite altimeters from 1992 to 2006 are provided by Aviso (http://www.aviso.oceanobs.com).

Hourly ocean velocities at four depths (50 m, 150 m, 350 m, and 750 m) in the Lombok Strait, Ombai Strait, Timor Passage, and Makassar Strait (black diamonds in Fig. 2) are obtained from the International Nusantara Stratification and Transport (INSTANT) program which was conducted from August 2003 to

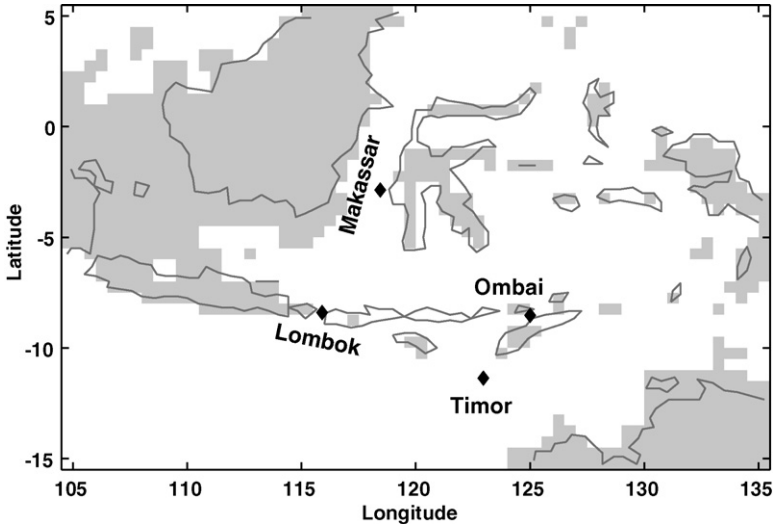

Fig. 2. INSTANT mooring positions in the Lombok Strait, the Ombai Strait, the Timor Passage, and the Makassar Strait. The shaded areas are the land-sea mask in SODA.

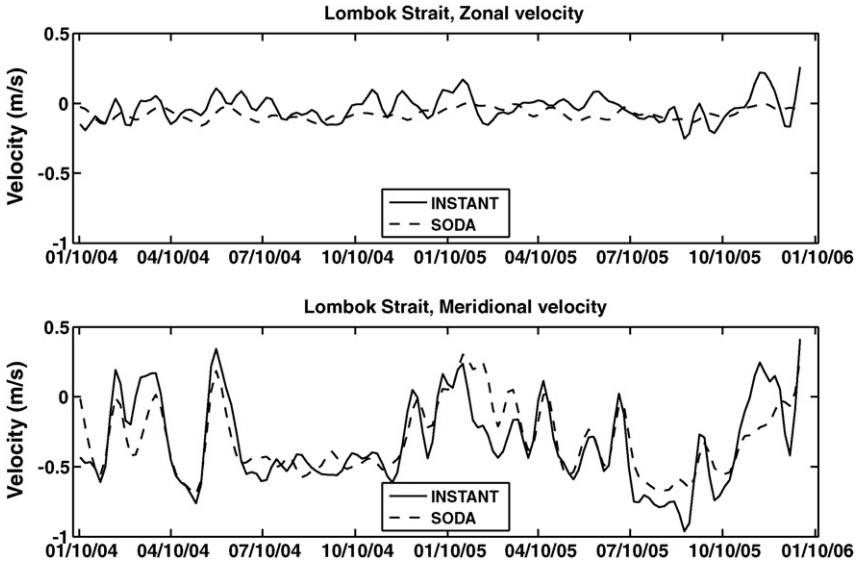

Fig. 3. Comparisons between INSTANT and SODA in the Lombok Strait at 50 m. The velocities are low-pass filtered with a cut-off period of 20 days. The correlation of zonal velocities is 0.30 and that of meridional velocities is 0.82.

the end of 2006 (Sprintall et al., 2004). Daily averaged temperature data are also obtained from the raw temperature measures in the INSTANT program, but at different depths in different straits. In order to show the spatial and interannual pattern of the MJO influence, the 5-day-average SODA products (Carton et al., 2000a,b; Carton and Giese, 2008) are also used in this study. Although SODA products were widely employed in previous studies of ITF (e.g., Potemra and Schneider, 2007; England and Huang, 2005), it is still necessary to compare SODA reanalysis with INSTANT data to ensure consistency of SODA products with independent observations, because the bottom topography and the coastlines in the assimilation model have obvious differences from reality (Fig. 2).

2.1. Comparisons of SODA to INSTANT data

The hourly INSTANT data are averaged every 5 days. In the Lombok Strait, the meridional velocity dominates. At 50 m, the meridional velocities from SODA agree well with the observations with a correlation of 0.82 (Fig. 3). The correlation of zonal currents, although small (0.3), is still statistically significant (Fig. 3). At 150 m, the correlation of meridional currents drops to 0.56 and that of zonal currents is 0.33 (not shown). In the deeper ocean (at 350 m and 750 m), the amplitudes of SODA are much smaller than the observations and the correlations are not statistically significant. In the Timor Passage, the zonal currents are dominant. As shown in Fig. 4, the SODA currents are somewhat less energetic than the currents recorded by INSTANT. The correlations of the zonal currents between SODA and INSTANT are 0.54 and 0.52 at 50 m and 150 m, respectively. But the correlations of the meridional velocities are not statistically significant. Again in the ocean deeper than 350 m, the SODA amplitudes are even smaller and the correlations with observations decrease. In the Makassar Strait, comparisons are very similar to those in Lombok Strait and Timor Passage. SODA can simulate the meridional current, which is the major component, in the upper 150 m (not shown), with a correlation of 0.57. But below that, the simulations do not compare favorably with INSTANT data. As for the Ombai Strait, the ocean-land masks (shades in Fig. 2) are notably different from reality (gray lines in Fig. 2). As a result, SODA in the Ombai Strait departs from the observations even at 50 m. Overall, SODA products are quite adequate as far as the major current components (e.g., the meridional currents in Lombok Strait, the zonal currents at the Timor passage, and the meridional currents in the Makassar Strait) are concerned in most channels of ITF in the upper 150 m. For current components that are tangential

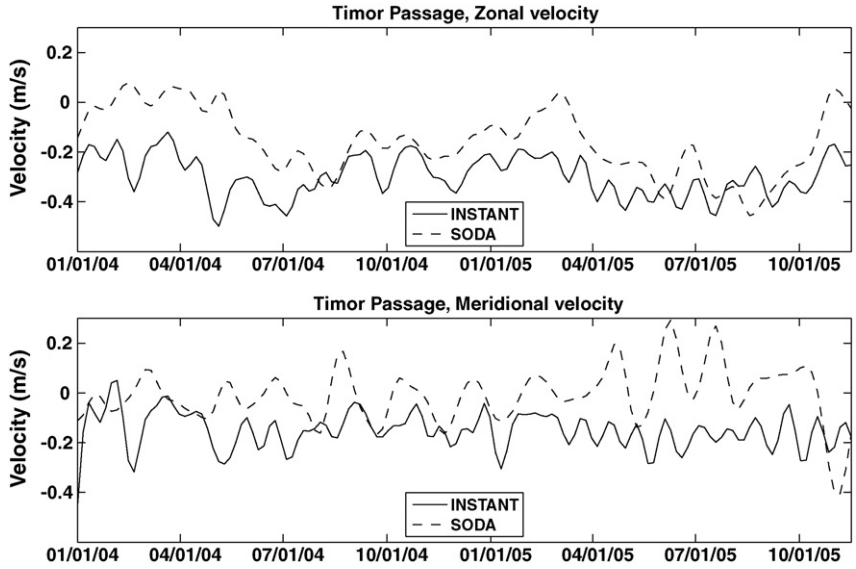

Fig. 4. The same as Fig. 3 but in the Timor Passage. The correlation of zonal velocities is 0.54 and that of meridional velocities is not statistically significant.

to the channels, SODA does not have high consistency with observations. Below 150 m, SODA is not able to adequately capture the observed currents in all channels, either. Therefore, in the following discussion, we mainly use the SODA products shallower than 150 m, which reliably reproduce the INSTANT observations.

3. MJO influence on the oceanic intraseasonal variability

3.1. Strength of the oceanic intraseasonal variability

The strength of the oceanic ISVs can be measured with the integral of the power spectrum density P, which is defined as

$$\bar{P}^2(\omega_1, \omega_2) = \int_{\omega_1}^{\omega_2} P\, d\omega,$$

where ω is the frequency. For the intraseasonal band, ω_1 is set to 1/20 day^{-1} and ω_2 is set to 1/90 day^{-1}. $\bar{P}$ is equivalent to the root-mean-square of the oceanic ISVs. As shown in Fig. 5a, intraseasonal SSTAs are about 0.35 °C in the eastern tropical Indian Ocean, which is smaller than those in the SEIO. This is partly attributable to the barrier layer in the tropical region which reduces the SST variations by decoupling the dynamic and thermodynamic processes in the mixed layer (the black contours in Fig. 5a; Murtugudde and Busalacchi, 1999; Schiller and Godfrey, 2003). However, the MJO footprint in the tropical oceanic ISVs can be seen from the intraseasonal SSH variabilities (Fig. 5b) and the intraseasonal variabilities in the thermocline, which is represented with the depth of the 20 °C isotherm (D20; Fig. 5c). In a model study, Annamalai et al. (2005) argued that the depth of 24 °C isotherm (D24), the typical position of the upper thermocline, is a better indicator to represent the cold entrainment into the upper mixed layer in the eastern tropical Indian Ocean than D20. With SODA reanalysis, the pattern of the intraseasonal D24 (not shown) is similar to that of the intraseasonal D20 shown in Fig. 5c. The variability induced by the MJOs accumulates against the Sumatran coast and propagates southward along the coast as Kelvin waves (Sprintall et al., 2000; Sengupta et al., 2001). As a result, one can see that significant intraseasonal SST anomalies (~0.5 °C), intraseasonal SSH anomalies (~6 cm),

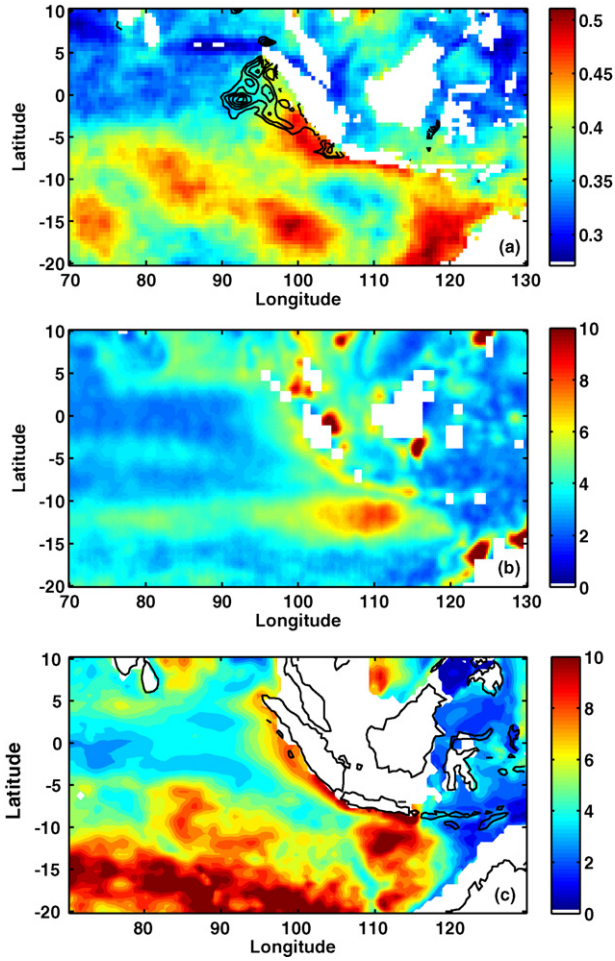

Fig. 5. $\overline{P}$ of intraseasonal SST anomalies (a), intraseasonal SSH anomalies (b), and intraseasonal D20 (c). The unit of SST anomalies is °C, the unit of SSH anomalies is cm, and the unit for D20 is m. The black contours in (a) are the barrier layer depths, starting from 16 m with an interval of 2 m.

and intraseasonal D20 variations (~10 m) are trapped along the Sumatran coast (Fig. 5). The enhanced oceanic ISVs due to the MJO forcing reach a maximum in the SEIO (between 10°S and 15°S), at the exit region of ITF. Hence, the MJO influence is one of the important contributors to the energetic oceanic ISVs in this region, in addition to the influence of the ITF and the internal oceanic instabilities (Feng and Wijffels, 2002; Yu and Potemra, 2006; Zhou et al., 2008).

3.2. *Intraseasonal oceanic response to MJOs*

Since MJOs have a distinct seasonality, i.e. they are strong in boreal winter but weak in boreal summer (Wang and Rui, 1990), the correlations between the MJO index and the intraseasonal SSTs are not statistically significant if data over all seasons are considered. The MJO index is composed of the first two leading PCs of the combined daily fields (Wheeler and Hendon, 2004). When PC1 is positive, deep convection happens over the maritime continent; when PC2 is negative, deep convection occurs in the tropical Indian Ocean. The details of the oceanic response to MJOs are obtained by examining the response to the two PCs, separately.

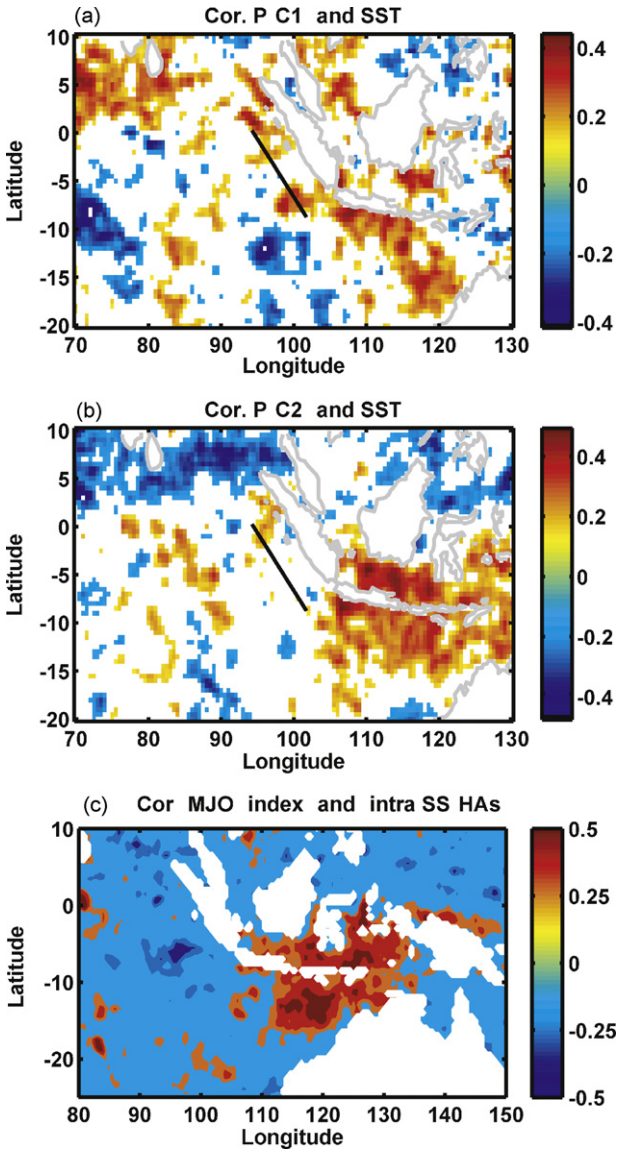

Fig. 6. (a) Correlation between significant daily PC1 (PC1 > 2) and the corresponding intraseasonal SST anomalies. (b) Correlation between distinct daily PC2 (PC2 < −2) and the corresponding intraseasonal SST anomalies. (c) Correlation between significant MJO events (MJO index > 2) and the intraseasonal SSH anomalies. The values in (b) are reversed, so that positive values represent sea surface warming and negative values represent sea surface cooling in both (a) and (b). Only statistically significant correlations at the 95% confidence level are shown.

The days with distinct daily PC1 which is larger than 2 and the days with distinct daily PC2 which is smaller than −2 are selected from 1993 to 2006. Correlations between PC1 (PC2) and the corresponding daily intraseasonal SST anomalies (obtained from gridded AVHRR data) for such events are shown in Fig. 6a (Fig. 6b). Note that because PC2 is negative, negative correlations between PC2 and the intraseasonal SST anomalies indicate sea surface warming associated with the strong convection in the tropical Indian Ocean, while positive correlations indicate sea surface cooling. In order to facilitate

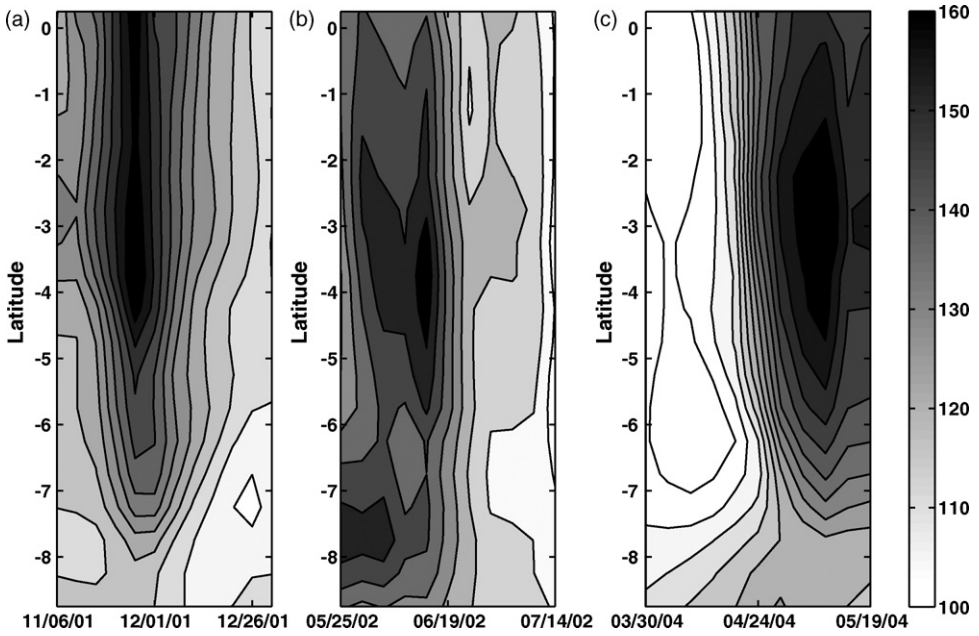

Fig. 7. Zonal mean D20 between the black lines in Fig. 6 and the western Sumatran coast. The unit is meter.

the comparison between Fig. 6a and b, the signs of correlations in Fig. 6b are reversed; so that all positive values in these two panels represent warming and all negative values represent cooling. In the eastern tropical Indian Ocean, especially between 10°N and the equator, the oceanic response to PC1 and PC2 are opposite. When deep convection occurs in the tropical Indian Ocean (i.e. PC2 < −2), which is in the convective-windy phase of MJOs, the short wave radiation is reduced due to heavy clouds and the latent heat loss increases due to enhanced surface winds. As a result, there is SST cooling over the eastern Indian Ocean. When the deep convection moves to the maritime continent (i.e. PC1 > 2), the eastern tropical Indian Ocean is in the clear-calm phase of MJOs. Hence, the downward solar radiation increases, latent heat flux decreases, producing warm SST anomalies. Therefore, the intraseasonal SST variations in the eastern tropical Indian Ocean between 10°N and the equator depend on the MJO phase and they are mainly attributable to the surface heat flux variations which are caused by the MJOs (Jones et al., 1998).

The oceanic response to MJOs is not restricted to the eastern tropical Indian Ocean but extends into the maritime continent. When deep convection occurs both in the tropical Indian Ocean (Fig. 6b) and over the maritime continent (Fig. 6a), there are significant positive (negative) correlations between PC1 (PC2) and the intraseasonal SST anomalies in the maritime continent, which represent warm SST anomalies associated with the MJOs. As discussed above, the convective-windy phase and the clear-calm phase of MJOs have opposite footprints on the surface heat fluxes. Therefore, the coherent SST anomalies in the two phases indicate that the MJO influence on the SST anomalies in the maritime continent is not solely dominated by surface heat fluxes but also oceanic processes (such as horizontal advection and entrainment heat flux, see details below) become important. The wind bursts associated with MJOs lead to downwelling equatorial Kelvin waves, which propagate poleward along the coasts after reaching the eastern boundary of the Indian Ocean (Sprintall et al., 2000; Valsala, 2008). In the southern hemisphere, the southward propagation along the Sumatran coast can be detected in D20 calculated with SODA products. Three typical cases are shown in Fig. 7. The patterns of the mixed layer depth variability, which is defined as the depth where the temperature is 0.5 °C cooler than the SSTs (Levitus, 1982) during the three MJO events, are similar to those of D20 shown in Fig. 7 (not shown). The thermocline and the mixed layer deepen due to the downwelling Kelvin waves. Although Kelvin

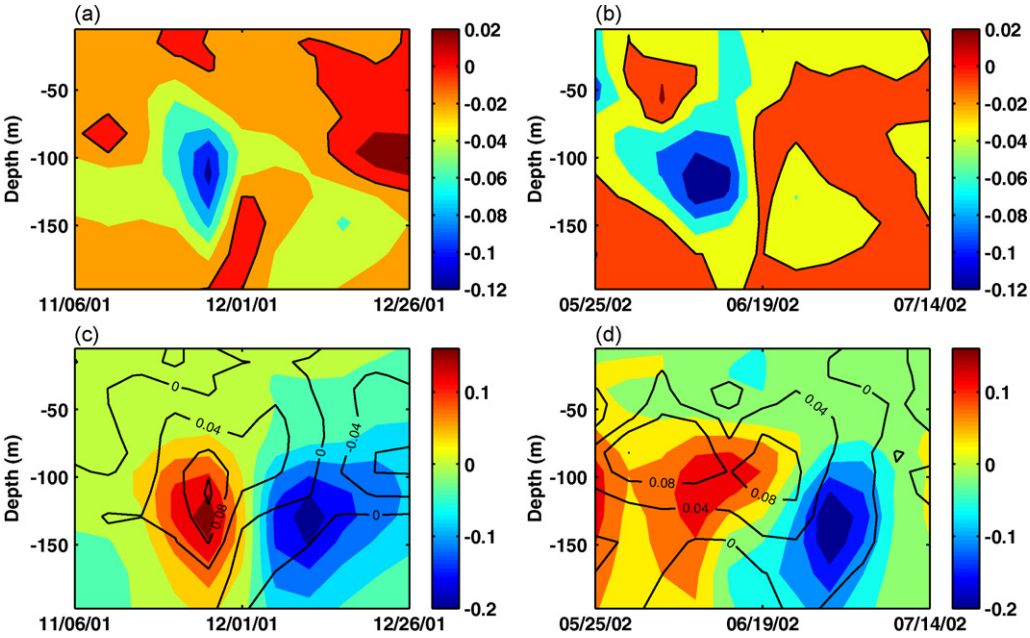

Fig. 8. (a) and (b): $V\partial T/\partial y$ averaged from 98°E to the western Sumatran coast during two MJO events. The black lines mark zero contours. Note that the negative values indicate southward warm advection. (c) and (d) The colors represent $\partial T/\partial t$ averaged from 5°S to 9°S and from 98°E to the western Sumatran coast. The contours show $(-V\partial T/\partial y\big|_{5°S}) - (-V\partial T/\partial y\big|_{9°S})$ averaged from 98°E to the western Sumatran coast. The unit is K/day.

waves propagate rapidly and SODA only has a time resolution of 5-day, the southward propagation from the equatorial region to the southeastern Indian Ocean is still detectable in Fig. 7. The speed can be roughly estimated to be around 2 m/s in a zoom-in figure of Fig. 7 (not shown), which is consistent with the speed of Kelvin waves calculated with $\sqrt{g'H}$ where g' is the reduced gravity and H is the mixed layer depth. At this speed, it only takes about 5 days to travel from the equator to the Lombok Strait (~9°S). This is why the southward propagation in Fig. 7 may not be very obvious. The thicker mixed layer associated with the surface convergence and deeper thermocline are accompanied by warm SST anomalies. These conclusions are consistent with the oceanic responses to the composite MJOs in the OGCM study of Waliser et al. (2003).

The meridional temperature advections $V\partial T/\partial y$ associated with the downwelling Kelvin waves during two MJO events are shown in Fig. 8a and b. Note that negative $V\partial T/\partial y$ indicates southward warm advection. Consequently, the sea water temperature increases, as shown with $\partial T/\partial t$ off the western Sumatran coast averaged from 5°S to 9°S (Fig. 8c and d). To facilitate a quantitative comparison, the differences of temperature advection at 5°S and 9°S off the western Sumatran coast (the net effect of the meridional advection on temperature variation) are superimposed in Fig. 8c and d. Both the warm advection and the temperature increase are more pronounced between 100 m and 150 m, which is approximately the depth of the mixed layer bottom. This is seen again later with INSTANT data. Comparing the contours and color codes in Fig. 8c and d, it is obvious that the warm meridional advection associated with the Kelvin waves due to the MJO influence is a dominant contributor to the temperature increases.

The correlations between the MJO events with MJO index larger than 2 and the intraseasonal SSH anomalies obtained from satellite altimetry are shown in Fig. 6c. Since the SSH variation is not large in the tropical region, due to the small Coriolis parameter, there are almost no significant correlations between the MJO index and the SSH anomalies. Hence, we do not calculate the correlations with PC1 and PC2 of MJOs separately, as we do in Fig. 6a and b. Significant correlations reside in the SEIO, which

is about 0.5. Moreover, positive correlations indicate the increase of SSH under the influence of MJOs, which is consistent with the deepening of the mixed layer and the thermocline due to the downwelling Kelvin waves, as discussed above and shown in Fig. 7. According to the correlations shown in Fig. 6, MJOs can explain about 20% variance of the oceanic ISVs in SST and SSH anomalies in the SEIO and the maritime continent. But considering the warm advection around the bottom of the upper layer (Fig. 8c and d), the downwelling Kelvin waves can contribute more than 20% in the subsurface layer. Thus, the estimate of 20% is conservative but reliable as far as the MJO influence on the oceanic ISVs in the SEIO and the maritime continents is concerned.

4. MJO influence on the ITF

As introduced above, the mass and heat fluxes of ITF vary on a wide temporal scale. In this study, we intend to focus on ITF variability related to the MJO influence on intraseasonal and interannual time scales.

4.1. MJOs and ITF at intraseasonal time scales

The ISVs account for 30–40% of the total ITF variance as shown in Fig. 9. Thus they are a non-negligible component of the ITF variability. Of course, not all ISVs of the ITF are attributable to the MJO influence. As discussed in the previous section, the MJO influence explains more than 20% of the ISVs in the SEIO. We will show below with the INSTANT data that both currents and temperatures have generally consistent responses to the MJO forcing during most MJO events.

There are 9 pronounced MJO events between 2004 and 2006 (marked with circles in Fig. 1) during the deployment of INSTANT moorings. Six out of the total 9 MJO events occurred in boreal winter

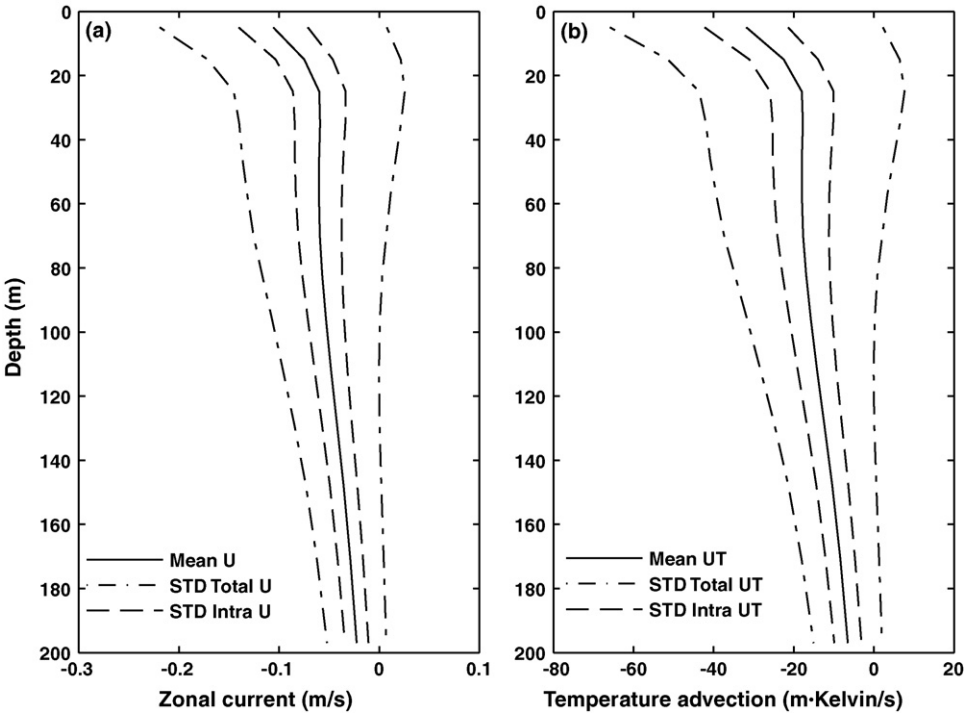

Fig. 9. (a) Mean zonal current (solid line), STD of the total zonal current (dot-dash lines), and STD of the intraseasonal zonal current (20–90 days; dash lines) averaged from 10°S to 15°S at 114°E. (b) The same as (a) but for temperature advection.

from December to May. One event occurred in July, one in September, and one in October. Although data for three years are not likely to be long enough to clearly resolve the seasonality of MJOs, it is still detectable that most MJO events occur in boreal winter. Generally, the patterns of negative OLR anomalies (representing strong convection) over the open Indian Ocean are similar among the 9 MJO events, regardless of their seasons. But the wind fields during summer MJOs and winter MJOs are expected to be different (see composites in Waliser et al., 2003, 2004). As a result, the MJOs signatures on SSTs are distinct for the winter and the summer. As a result, there can be differences of the MJO influence on SSTs between the winter and the summer (e.g., Duncan and Han, 2009; Duvel et al., 2004; Han et

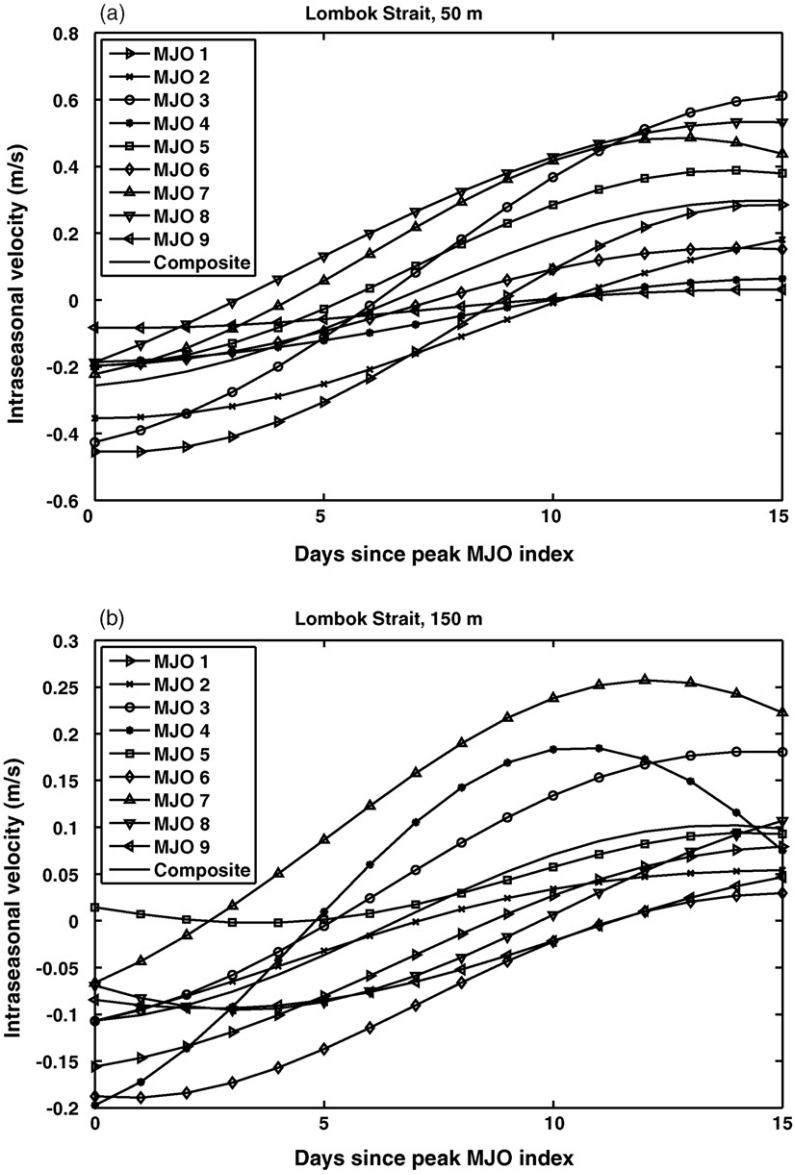

Fig. 10. Intraseasonal meridional currents at 50 m (a) and 150 m (b) in the Lombok Strait. The zeroth day is the day with a peak MJO index, which are marked with circles in Fig. 1.

al., 2007; Vinayachandran and Saji, 2008). However, with only 9 MJO events, it is hard to draw robust conclusions here on the seasonal difference in the MJO impacts. Therefore, in the following study, we only examine the common oceanic responses to all MJO events without separating the seasons.

The ITF tends to be reduced by the southward propagating downwelling Kelvin waves generated by the MJOs near the equator (Fig. 7). In the Lombok Strait, the meridional currents are consistently reversed from southward to northward at 50 m in 15 days after the day with a peak MJO index (Fig. 10a). At 150 m, the composite meridional velocity of the 9 MJO events is also reversed (Fig. 10b). In the Ombai Strait, although the composite zonal currents reverse from westward to eastward, the zonal currents

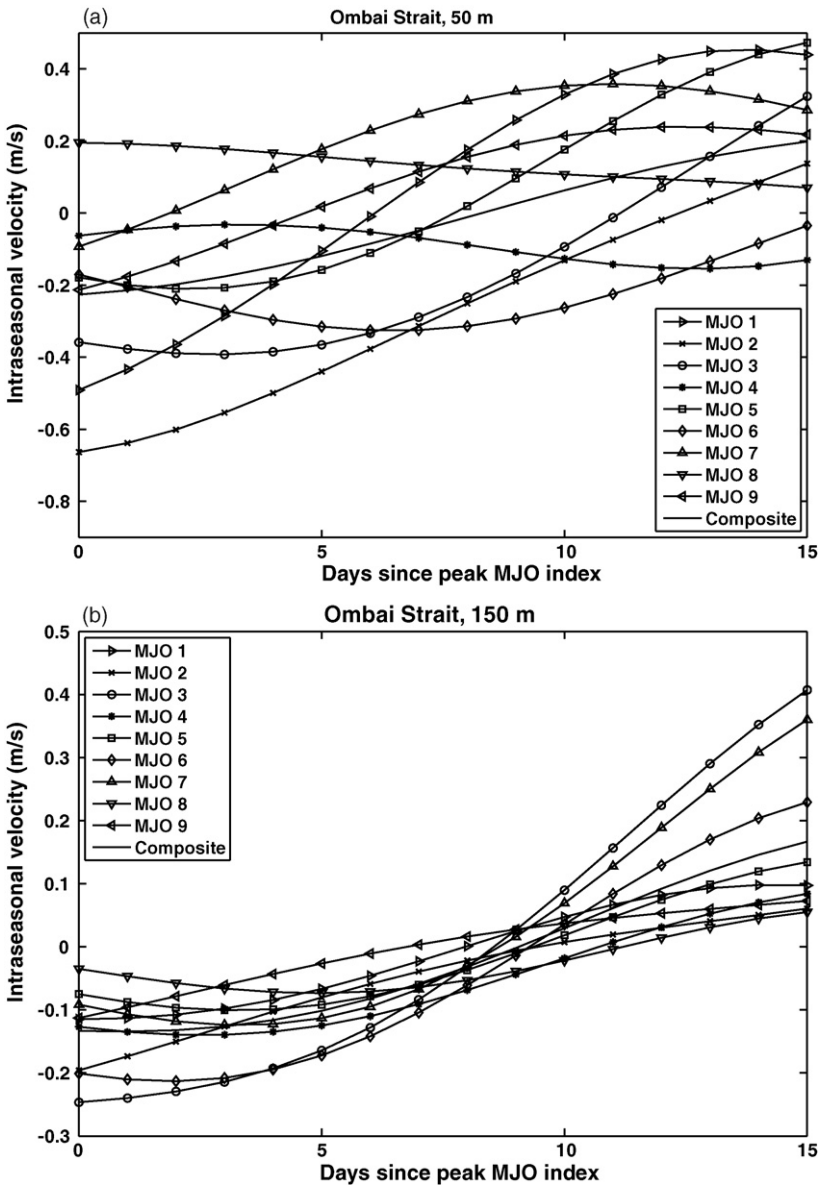

Fig. 11. Intraseasonal zonal currents at 50 m (a) and 150 m (b) in the Ombai Strait. The zeroth day is the day with a peak MJO index, which are marked with circles in Fig. 1.

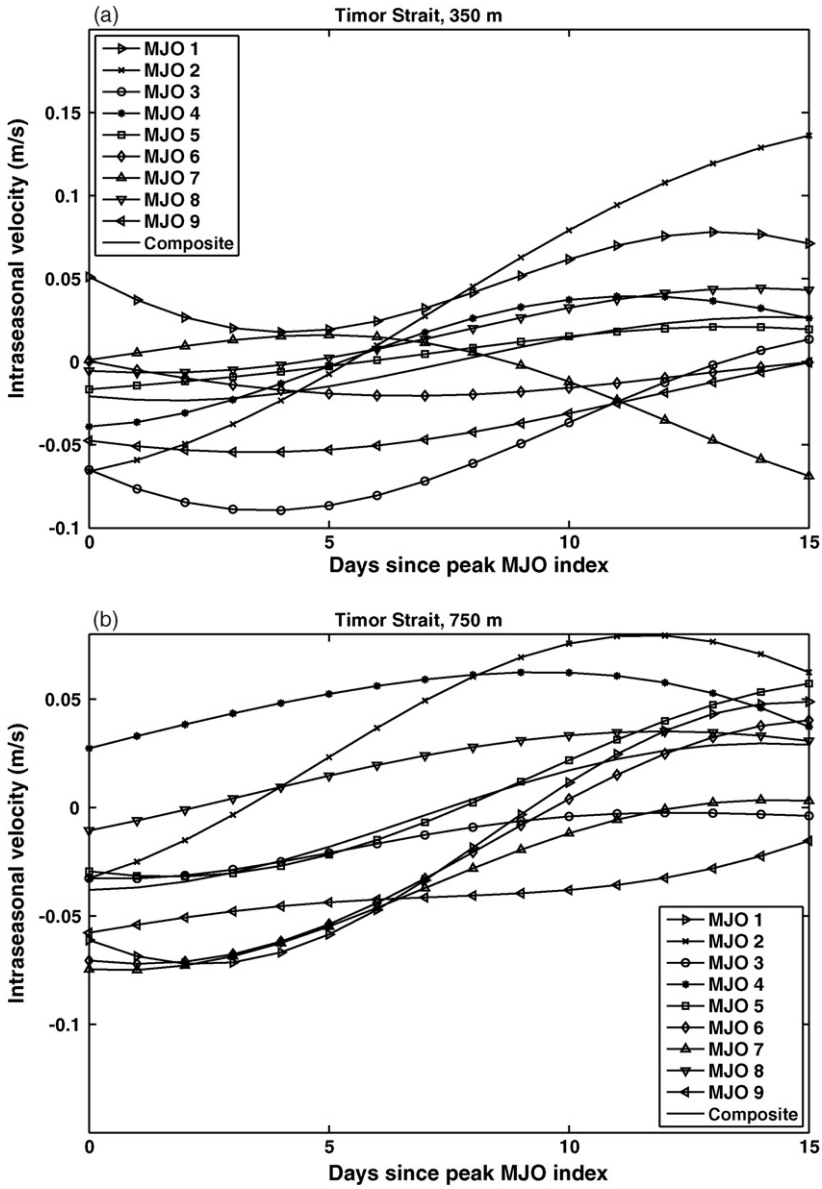

Fig. 12. Intraseasonal zonal currents at 50 m (a) and 150 m (b) in the Timor Passage. The zeroth day is the day with a peak MJO index, which are marked with circles in Fig. 1.

during the 9 MJO events are not very consistent (Fig. 11a). However, at 150 m, one can see consistent reduction of westward zonal current associated with the MJO events (Fig. 11b). In the Timor Passage, which is the major pathway for the ITF, the MJO influence via the downwelling Kelvin waves can be detected only in the deeper ocean (Fig. 12). At 50 m and 150 m, there are no consistent intraseasonal variabilities in zonal currents associated with the 9 pronounced MJO events. However, at 350 m, the westward zonal currents are reduced and the composite current is reversed to eastward. One exception is the zonal current during MJO event 7 (marked with Δ in Fig. 12a), which first turns slightly

eastward but becomes westward 5 days after the peak MJO. The peak of MJO 7 occurs on September 9, 2005, when the ITF reaches a maximum. Thus the ISVs due to strong ITF overwhelm the MJO influence on the intraseasonal zonal currents in the Timor Passage (not all ISVs are attributable to MJOs as argued above), so that they are not consistent with the ISVs during the other MJO events. Another notable feature in the Timor Strait is that the response to MJO events is detectable as far down as 750 m (Fig. 12b), which is not found in the other two straits. Thus the downwelling Kelvin waves can propagate to the deeper ocean along the Sumatran coast to about 12°S. With the high-resolution Argo data, Matthews et al. (2007) found that the influence of MJOs can propagate as deep as 1500 m in the tropical Pacific Ocean (between 5°N and 5°S) by triggering the downward propagating equatorial Kelvin waves and proposed that the deep ocean responses to MJOs can propagate to extra-tropical regions. In the Indian Ocean, the MJO influence can also reach 750 m around 12°S. The unresolved issue is whether the MJO-induced downwelling Kelvin waves can cross the Timor Passage and continue to propagate along the western Australian coast to the mid-latitudes and to even deeper ocean (e.g., the observational and numerical studies by Qiu et al. (1999) and Sprintall et al. (2000); the theoretical studies by Durland and Qiu (2003) and Johnson and Garrett (2006)). This cannot be resolved without further observations and high-resolution model studies. As for the Makassar Strait, there is no obviously consistent response to the 9 MJO events, because the inflow in this strait is mainly from the Pacific Ocean.

The intraseasonal water temperature anomalies in the Ombai Strait during the 9 MJO events from 2004 to 2006 are shown in Fig. 13. As shown in Fig. 8, the core of warm advection is between 100 m

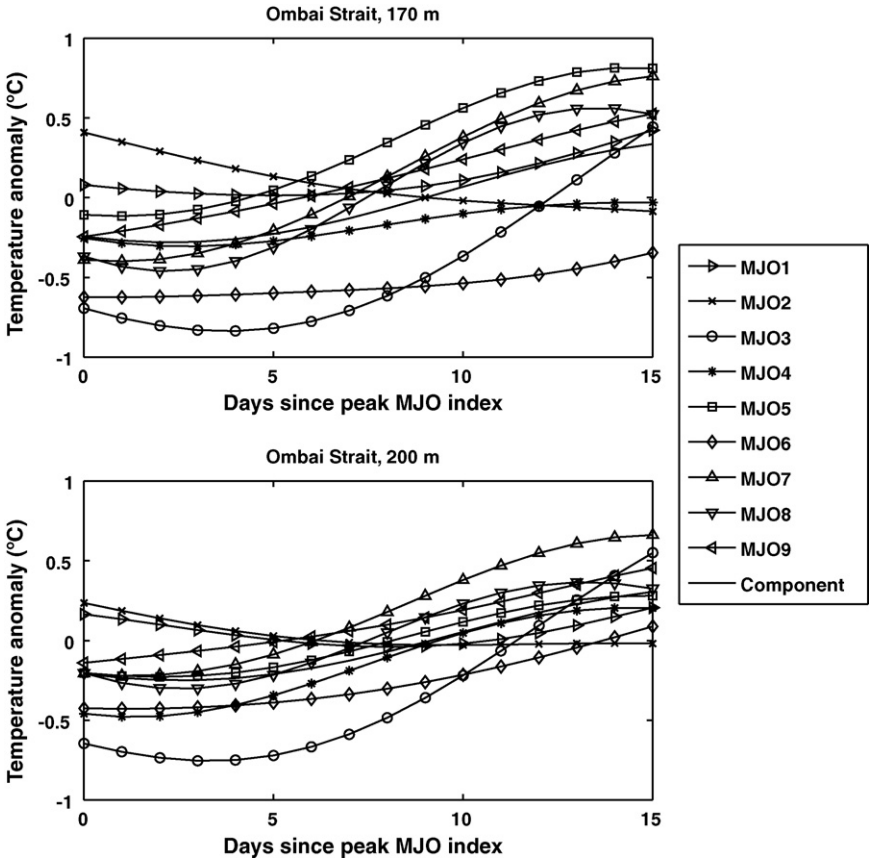

Fig. 13. Intraseasonal temperature anomalies during the 9 MJO events in the Ombai Strait. The zeroth day is the day with a peak MJO index, which are marked with circles in Fig. 1.

and 150 m off the Sumatran coast. At the Ombai Strait, the influence of the downwelling Kelvin waves goes a little deeper. Consequently, at 170 m and 200 m in the Ombai Strait, the sea water temperatures increase by about 0.4 °C. At 100 m and 550 m, there are no significant temperature anomalies for the composite MJO events. This is also attributable to the persistent northward flow, which is from the Indian Ocean to the Banda Sea, especially in the northern Ombai Strait (Sprintall et al., 2009). Therefore, the downwelling Kelvin waves from the Indian Ocean do not change the heat budget at these two depths and the sea water temperatures do not change significantly. The two depths of 100 m and 550 m can mark the approximate upper and lower boundaries of the influence of downwelling Kelvin waves around the Ombai Strait. In the Lombok Strait, temperatures also increase as a response to MJOs in the upper 200 m, which is a consistent depth to which the response of ocean currents to MJOs is discernible. But the temperature responses are not as consistent as the ones in the Ombai Strait. In the Timor Strait, although some MJO influences are detected at as deep as 750 m, the MJO influence on the temperature in the deep ocean is not clear. Thus, the figures in the latter two straits are not shown.

4.2. MJOs and ITF at interannual time scales

We also explored the interannual relations between the MJOs and the ITF using the SODA products. As shown with the comparisons between SODA and INSTANT (Section 2), SODA captures the dominant ocean currents well in waters shallower than 150 m. The ITF variation can be estimated with the mean zonal velocities averaged between 10°S and 15°S at 114°E from SODA. A similar measure of ITF was employed in Murtugudde et al. (1998), Potemra and Schneider (2007), and England and Huang (2005). The correlation between the 5-day mean MJO index and zonal velocities reaches a maximum at the surface and decreases with depth (Fig. 14a). Note that positive correlations indicate that strong MJOs

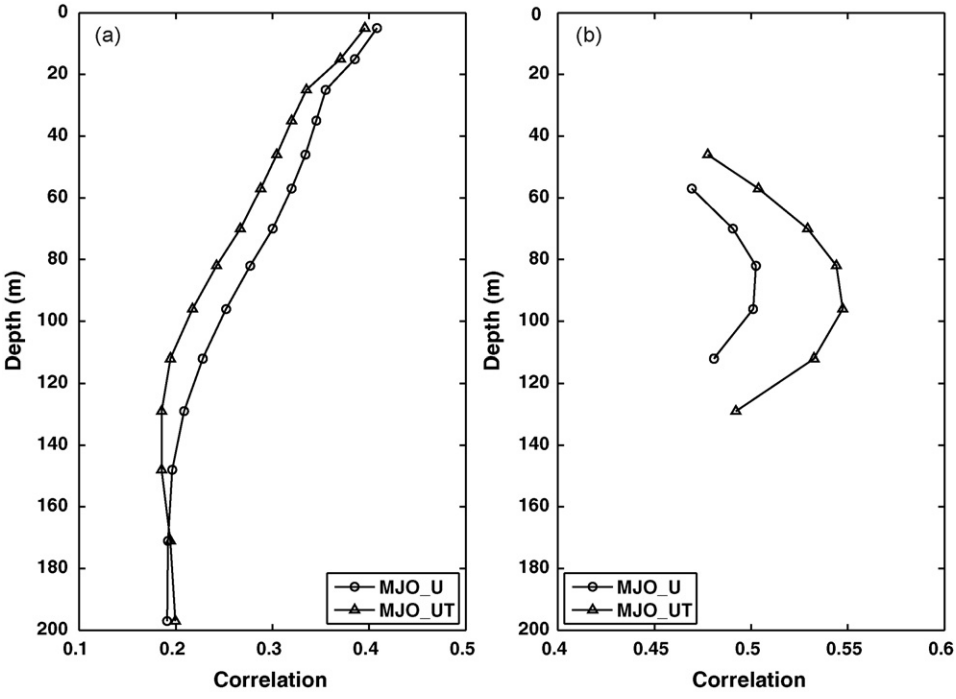

Fig. 14. (a) Correlations between the 5-day MJO index and the zonal velocity, as well as correlations between the 5-day MJO index and zonal temperature advection. (b) Correlations between the annual MJO index and the annual mean zonal velocity, as well as correlations between the annual MJO index and annual mean temperature advection. The zonal velocity and temperature advection are averaged between 10°S and 15°S at 114°E. The correlations are statistically significant at a confidence level of 95%.

lead to weak ITF, since the ITF is westward (negative velocities). This is consistent with the above results obtained from the INSTANT data. A similar vertical structure can be seen in the correlations between the 5-day mean MJO index and the zonal temperature advection, which is calculated as the product of zonal velocities and temperatures (Fig. 14a). Therefore, MJOs can reduce the ITF and the associated temperature advection.

Besides the seasonal impacts, MJOs also influence the interannual variability of ITF. Because MJOs are typically dominant in boreal winter, the annual mean MJO index is much smoother than the monthly mean MJO. The maximum monthly MJO index of each year is selected to represent the MJO strength of that year, which is referred to as the annual MJO index hereafter. The correlations between the annual MJO index and the mean ITF and temperature advection of each year are statistically significant at a 95% confidence level only around the bottom of upper mixed layer (centered at 100 m), at zero lag between MJOs and ITF (Fig. 14b). The positive correlations confirm again that in the strong (weak) MJO years, the annual mean ITF tends to be weaker (stronger). However, the relation between significant MJOs in boreal winter and strong ITF in boreal summer is relatively weak. When maximum ITF and the associated temperature advection of each year during boreal summer are considered, there is no significant correlation at 95% confidence level indicating that MJOs do not have a pronounced impact on the annual peak in ITF. However, if the confidence level is reduced to 90%, their correlations become significantly positive with a vertical structure similar to Fig. 14b (not shown). Therefore, MJOs tend to slightly reduce the ITF peak in boreal summer.

5. Discussion and conclusion

The MJO influence on the eastern Indian Ocean and the maritime continent is studied with satellite and mooring observations as well as SODA reanalysis. The oceanic ISVs are a direct response to the atmospheric intraseasonal forcing. In the tropical eastern Indian Ocean, SSTs have different responses to different phases of MJOs. When deep convection occurs in the tropical Indian Ocean, there is an SST cooling and when the convection moves to the maritime continent, warm SST anomalies are established. The opposite responses are attributable to contrasting surface heat flux variation, which is induced by the MJOs. The strong winds associated with the MJOs lead to downwelling equatorial Kelvin waves. When they reach the eastern coast of the Indian Ocean, they propagate southward along the Sumatran coast, leading to a deepening of the thermocline in the SEIO. As a result, the entrainment cooling of the SSTs is reduced generating relatively warm SST anomalies. Considering the high mean SSTs, even small SST warming is significant in terms of atmospheric or coupled responses (Palmer and Mansfield, 1984). The MJO influence is one of the major components of the intraseasonal SST and SSH anomalies in the SEIO, which contribute no less than 20% to the total oceanic ISVs. Because the SEIO is the exit region of ITF, MJOs can reduce the annual mean ITF and the associated temperature advection. However, MJOs have only a weak impact on peak ITF in boreal summer.

Waliser et al. (2003) suggested that the MJO-related low-frequency variations can probably influence the evolution of the Indian Ocean Dipole/Zonal Mode (IODZM; also see Murtugudde et al., 2000). Ashok et al. (2004) found that decadal variation of IODZM and decadal ENSO variation are not well correlated, which led them to conjecture that the former is attributable to the low-frequency modulation of the interannual variability. The modulation of annual mean ITF and the temperature advection by the MJOs is likely to introduce a low-frequency interannual variability in the Indian Ocean, which can potentially contribute to the decadal variation of IODZM. However, due to a lack of sufficiently long time-series of observations (e.g., longer than 20 years), this hypothesis can only be tested with an elaborately designed model at present. The results presented here do emphasize the role of reliable data such as those from INSTANT in greatly enhancing understanding of key processes and the need for continued efforts for sustained observations.

Acknowledgements

This work was supported by NASA Earth System Science Fellowship and NASA Indian Ocean Mesoscale Funding. We are thankful to two anonymous reviewers for their insightful comments,

which help to improve the manuscript significantly. We deeply appreciate James Carton for providing the 5-day SODA products.

References

Annamalai, H., Potemra, J., Murtugudde, R., McCreary, J.P., 2005. Effect of preconditioning on the extreme climate events in the tropical Indian Ocean. Journal of Climate 18, 3450–3469.
Ashok, K., Chan, W.L., Motoi, T., Yamagata, T., 2004. Decadal variability of the Indian Ocean dipole. Geophysical Research Letters, 31.
Carton, J.A., Giese, B.S., 2008. A reanalysis of ocean climate using Simple Ocean Data Assimilation (SODA). Monthly Weather Review 136, 2999–3017.
Carton, J.A., Chepurin, G., Cao, X.H., 2000a. A Simple Ocean Data Assimilation analysis of the global upper ocean 1950–1995. Part II. Results. Journal of Physical Oceanography 30, 311–326.
Carton, J.A., Chepurin, G., Cao, X.H., Giese, B., 2000b. A Simple Ocean Data Assimilation analysis of the global upper ocean 1950–1995. Part I. Methodology. Journal of Physical Oceanography 30, 294–309.
Duncan, B., Han, W.Q., 2009. Indian Ocean intraseasonal sea surface temperature variability during boreal summer: Madden–Julian Oscillation versus submonthly forcing and processes. Journal of Geophysical Research-Oceans, 114.
Durland, T.S., Qiu, B., 2003. Transmission of subinertial Kelvin waves through a strait. Journal of Physical Oceanography 33, 1337–1350.
Duvel, J.P., Roca, R., Vialard, J., 2004. Ocean mixed layer temperature variations induced by intraseasonal convective perturbations over the Indian Ocean. Journal of the Atmospheric Sciences 61, 1004–1023.
England, M.H., Huang, F., 2005. On the interannual variability of the Indonesian Throughflow and its linkage with ENSO. Journal of Climate 18, 1435–1444.
Feng, M., Wijffels, S., 2002. Intraseasonal variability in the south equatorial current of the east Indian Ocean. Journal of Physical Oceanography 32, 265–277.
Ffield, A., Gordon, A.L., 1992. Vertical mixing in the Indonesian thermocline. Journal of Physical Oceanography 22, 184–195.
Gordon, A.L., 2001. Interocean exchange. In: Siedler, G., et al. (Eds.), Ocean Circulation and Climate. Academic Press, pp. 303–314.
Godfrey, J.S., 1996. The effect of the Indonesian throughflow on ocean circulation and heat exchange with the atmosphere: a review. Journal of Geophysical Research-Oceans 101, 12217–12237.
Han, W.Q., Yuan, D.L., Liu, W.T., Halkides, D.J., 2007. Intraseasonal variability of Indian Ocean sea surface temperature during boreal winter: Madden–Julian Oscillation versus submonthly forcing and processes. Journal of Geophysical Research-Oceans, 112.
Hatayama, T., Awaji, T., Akitomo, K., 1996. Tidal currents in the Indonesian Seas and their effect on transport and mixing. Journal of Geophysical Research-Oceans 101, 12353–12373.
Hautala, S.L., Reid, J.L., Bray, N., 1996. The distribution and mixing of Pacific water masses in the Indonesian Seas. Journal of Geophysical Research-Oceans 101, 12375–12389.
Hautala, S.L., Sprintall, J., Potemra, J.T., Chong, J.C., Pandoe, W., Bray, N., Ilahude, A.G., 2001. Velocity structure and transport of the Indonesian Throughflow in the major straits restricting flow into the Indian Ocean. Journal of Geophysical Research-Oceans 106, 19527–19546.
Iskandar, I., Tozuka, T., Sasaki, H., Masumoto, Y., Yamagata, T., 2006. Intraseasonal variations of surface and subsurface currents off Java as simulated in a high-resolution ocean general circulation model. Journal of Geophysical Research-Oceans, 111.
Johnson, H.L., Garrett, C., 2006. What fraction of a Kelvin wave incident on a narrow strait is transmitted? Journal of Physical Oceanography 36, 945–954.
Jones, C., Waliser, D.E., Gautier, C., 1998. The influence of the Madden–Julian oscillation on ocean surface heat fluxes and sea surface temperature. Journal of Climate 11, 1057–1072.
Kalnay, E., Coauthors, 1996. The NCEP/NCAR 40-Year Reanalysis Project. Bulletin of the American Meteorological Society 77, 437–471.
Kessler, W.S., McPhaden, M.J., Weickmann, K.M., 1995. Forcing of intraseasonal Kelvin waves in the equatorial pacific. Journal of Geophysical Research-Oceans 100, 10613–10631.
Levitus, S., 1982. Climatological Atlas of the World Ocean. NOAA Professional Paper 13. U.S. Department of Commerce, Sydney.
Liebmann, B., Smith, C.A., 1996. Description of a complete (interpolated) outgoing longwave radiation dataset. Bulletin of the American Meteorological Society 77, 1275–1277.
Masumoto, Y., 2002. Effects of interannual variability in the eastern Indian Ocean on the Indonesian throughflow. Journal of Oceanography 58, 175–182.
Matthews, A.J., Singhruck, P., Heywood, K.J., 2007. Deep ocean impact of a Madden–Julian Oscillation observed by Argo floats. Science 318, 1765–1769.
McClain, E.P., Pichel, W.G., Walton, C.C., 1985. Comparative performance of Avhrr-Based multichannel sea-surface temperatures. Journal of Geophysical Research-Oceans 90, 1587–1601.
Meyers, G., 1996. Variation of Indonesian throughflow and the El Nino Southern Oscillation. Journal of Geophysical Research-Oceans 101, 12255–12263.
Meyers, G., Bailey, R.J., Worby, A.P., 1995. Geostrophic transport of Indonesian throughflow. Deep-Sea Research I 42, 1163–1174.
Milliff, R.F., Morzel, J., Chelton, D.B., Freilich, M.H., 2004. Wind stress curl and wind stress divergence biases from rain effects on QSCAT surface wind retrievals. Journal of Atmospheric and Oceanic Technology 21, 1216–1231.
Murtugudde, R., Busalacchi, A.J., Beauchamp, J., 1998. Seasonal-to-interannual effects of the Indonesian throughflow on the tropical Indo-Pacific Basin. Journal of Geophysical Research-Oceans 103, 21425–21441.
Murtugudde, R., McCreary, J.P., Busalacchi, A.J., 2000. Oceanic processes associated with anomalous events in the Indian Ocean with relevance to 1997–1998. Journal of Geophysical Research-Oceans 105, 3295–3306.
Murtugudde, R., Busalacchi, A.J., 1999. Interannual variability of the dynamics and thermodynamics of the tropical Indian Ocean. Journal of Climate 12, 2300–2326.

Palmer, T.N., Mansfield, D.A., 1984. Response of 2 atmospheric general-circulation models to sea-surface temperature anomalies in the Tropical East and West Pacific. Nature 310, 483–485.
Potemra, J.T., Schneider, N., 2007. Interannual variations of the Indonesian throughflow. Journal of Geophysical Research-Oceans, 112.
Potemra, J.T., Hautala, S.L., Sprintall, J., Pandoe, W., 2002. Interaction between the Indonesian Seas and the Indian Ocean in observations and numerical models. Journal of Physical Oceanography 32, 1838–1854.
Qiu, B., Mao, M., Kashino, Y., 1999. Intraseasonal variability in the indo-pacific throughflow and the regions surrounding the Indonesian seas. Journal of Physical Oceanography 29, 1599–1618.
Reppin, J., Schott, F.A., Fischer, J., Quadfasel, D., 1999. Equatorial currents and transports in the upper central Indian Ocean: annual cycle and interannual variability. Journal of Geophysical Research-Oceans 104, 15495–15514.
Schiller, A., Godfrey, J.S., 2003. Indian Ocean intraseasonal variability in an ocean general circulation model. Journal of Climate 16, 21–39.
Sengupta, D., Senan, R., Goswami, B.N., 2001. Origin of intraseasonal variability of circulation in the tropical central Indian Ocean. Geophysical Research Letters 28, 1267–1270.
Simmons, A.J., Gibson, J.K. (Eds.), 2000. The ERA-40 Project Plan. ERA-40 Project Report Series 1, 62 pp.
Sprintall, J., Gordon, A.L., Murtugudde, R., Susanto, R.D., 2000. A semiannual Indian Ocean forced Kelvin wave observed in the Indonesian seas in May 1997. Journal of Geophysical Research-Oceans 105, 17217–17230.
Sprintall, J., Wijffels, S., Gordon, A.L., Ffield, A., Molcard, R., Susanto, R.D., Soesilo, I., Sopaheluwakan, J., Surachman, Y., van Aken, H.M., 2004. INSTANT: a new international array to measure the Indonesian Throughflow. EOS 85, 39.
Sprintall, J., Wijffels, S.E., Molcard, R., Jaya, I., 2009. Direct estimates of the Indonesian Throughflow entering the Indian Ocean: 2004–2006. Journal of Geophysical Research-Oceans, 114.
Susanto, R.D., Gordon, A.L., 2005. Velocity and transport of the Makassar Strait throughflow. Journal of Geophysical Research-Oceans, 110.
Valsala, V., 2008. First and second baroclinic mode responses of the tropical Indian Ocean to interannual equatorial wind anomalies. Journal of Oceanography 64, 479–494.
Vinayachandran, P.N., Saji, N.H., 2008. Mechanisms of South Indian Ocean intraseasonal cooling. Geophysical Research Letters, 35.
Vranes, K., Gordon, A.L., Ffield, A., 2002. The heat transport of the Indonesian Throughflow and implications for the Indian Ocean heat budget. Deep-Sea Research Part II 49, 1391–1410.
Waliser, D.E., Murtugudde, R., Lucas, L.E., 2003. Indo-Pacific Ocean response to atmospheric intraseasonal variability. 1. Austral summer and the Madden–Julian Oscillation. Journal of Geophysical Research-Oceans, 108.
Waliser, D.E., Murtugudde, R., Lucas, L.E., 2004. Indo-Pacific Ocean response to atmospheric intraseasonal variability. 2. Boreal summer and the Intraseasonal Oscillation. Journal of Geophysical Research-Oceans, 109.
Wang, B., Rui, H., 1990. Synoptic climatology of transient tropical intraseasonal convection anomalies – 1975–1985. Meteorology and Atmospheric Physics 44, 43–61.
Wheeler, M.C., Hendon, H.H., 2004. An all-season real-time multivariate MJO index: development of an index for monitoring and prediction. Monthly Weather Review 132, 1917–1932.
Wijffels, S., Meyers, G., 2004. An intersection of oceanic waveguides: variability in the Indonesian throughflow region. Journal of Physical Oceanography 34, 1232–1253.
Woolnough, S.J., Slingo, J.M., Hoskins, B.J., 2000. The relationship between convection and sea surface temperature on intraseasonal timescales. Journal of Climate 13, 2086–2104.
Yoneyama, K., Masumoto, Y., Kuroda, Y., Katsumata, M., Mizuno, K., Takayabu, Y.N., Yoshizaki, M., Shareef, A., Fujiyoshi, Y., McPhaden, M.J., Murty, V.S.N., Shirooka, R., Yasunaga, K., Yamada, H., Sato, N., Ushiyama, T., Moteki, Q., Seiki, A., Fujita, M., Ando, K., Hase, H., Ueki, I., Horii, T., Yokoyama, C., Miyakawa, T., 2008. Mismo field experiment in the equatorial Indian Ocean. Bulletin of the American Meteorological Society 89, 1889–1903.
Yu, Z., Potemra, J., 2006. Generation mechanism for the intraseasonal variability in the Indo-Australian basin. Journal of Geophysical Research-Oceans, 111.
Zhou, L., Murtugudde, R., Jochum, M., 2008. Dynamics of the intraseasonal oscillations in the Indian Ocean South Equatorial Current. Journal of Physical Oceanography 38, 121–132.